

Supplementary Appendix

This appendix has been provided by the authors to give readers additional information about their work.

Supplement to: Margolin DH, Kousi M, Chan Y-M, et al. Ataxia, dementia, and hypogonadotropism caused by disordered ubiquitination. *N Engl J Med* 2013;368:1992-2003. DOI: 10.1056/NEJMoa1215993

Table of Contents

Supplementary Methods	2
Figure S1. Schematic of the <i>RNF216</i> and <i>OTUD4</i> genes and encoded proteins	5
Figure S2. Allele-specific RT-PCR of <i>RNF216</i>	6
Figure S3. Efficiency of the <i>rnf216</i> and <i>otud4</i> morpholinos	7
Figure S4. Microphthalmia with knockdown of <i>rnf216</i> and <i>otud4</i>	8
Table S1. Homozygous variants found in Subject 3	9
Table S2. Laboratory and genetic results for subjects	10
Table S3. IHH and ataxia genes used for interaction analyses	11
Table S4. Primers for allele-specific PCR	12
References	13

Supplementary Methods

Exome capture and sequencing

Whole-exome sequencing for Subject 3 was performed through the Mendelian Sequencing Consortium at the Broad Institute. Exomic DNA was captured using the Agilent SureSelect Human All Exon v2, and the captured libraries were sequenced using an Illumina HiSeq 2000. The reads were mapped to the hg19 reference genome using the Burrows–Wheeler alignment (BWA) algorithm,¹ and both indel and single nucleotide variant calling were performed using the Genome Analysis Toolkit (GATK).²

Identification and analysis of candidate genes and variants

Variants were filtered using the standard GATK filters, read depth $\geq 10x$ and genotype quality score ≥ 30 . In addition, homozygous variants with $>10\%$ of the alternate reads and heterozygous variants with allele balance $<30\%$ or $>70\%$ of the alternate reads were filtered away to ensure specificity of the re-alignment. Homozygous single nucleotide variants that were found in Patient 3, present at less than 1% frequency in the NHLBI GO Exome Sequencing Project (ESP),³ and predicted to be damaging by PolyPhen2,⁴ as well as homozygous insertions and deletions that were present at less than 1% in a set of 378 control exomes, were Sanger sequenced in the remaining siblings and one parent from the index pedigree. Variants that exhibited proper segregation were then sequenced in additional family members from the index pedigree as well as in another seven unrelated probands with Gordon Holmes syndrome and three affected family members of these probands. SIFT,⁵ PANTHER,⁶ and Mutation Taster⁷ were used to further support the predicted pathogenicity of the variants. Nonsense and essential splice-site mutations in the ESP were considered overtly deleterious, and missense mutations present at $<1\%$ frequency and predicted to be pathogenic by the four prediction programs were considered likely deleterious. DAPPLE,⁸ Grail,⁹ Endeavour,¹⁰ InWeb scored network,¹¹ and CNVconnect¹² were used to identify potential interactions among *RNF216*, *OTUD4*, and other known ataxia or hypogonadotropic hypogonadism genes (Table S3).

Allele-specific RT-PCR

Total RNA was extracted from lymphoblast cell lines for Subjects 5-7 and their parents using the RNeasy Kit (Qiagen). First-strand cDNA was synthesized with oligo-dT primers using the SuperScript III First Strand Synthesis System (Invitrogen). Quantitative real-time polymerase chain reaction (PCR) was performed on an ABI 7000 Real-Time PCR System by Dr. Victoria Petkova at the Beth Israel Deaconess Medical Center TaqMan Core. Primers are listed in Table S4; primers for human *GAPDH* were purchased from ABI. All reactions were performed in duplicate in separate wells, and the resulting C_t 's were normalized to that of *GAPDH*.

Reproductive Endocrine Phenotyping

Subjects 2, 6, and 8 underwent blood sampling every 10-15 minutes for 3.25-12 h to examine the frequency, amplitude, and morphology of endogenous GnRH-induced luteinizing hormone (LH) pulse patterns. Pulses of LH secretion were identified using a modified version of the method of Santen and Bardin.¹³⁻¹⁴ Subjects 1, 2, 6, and 8 received exogenous, pulsatile GnRH with monitoring of gonadotropin responses as described previously.¹⁵⁻¹⁶ Hormone assays were performed as described in ref. 16; the Second International Reference Preparation was used as the standard for LH and FSH.

Morpholino oligonucleotide design

Morpholino oligonucleotides were obtained from Gene Tools, LLC (Philomath, OR, USA). Reciprocal BLAST against the zebrafish genome identified a sole zebrafish ortholog of *RNF126* (ENSDARG00000087893, 59% similarity, 46% identity). The antisense MO used for the silencing of zebrafish *rnf216* targeted the intron 5' donor splice site of the gene: CAGAAAATAGTTTGTGCTTACACAT.

Similar to *rnf216*, a sole ortholog of the human transcript for *OTUD4* was identified in zebrafish (73% similarity, 61% identity). Although genomic annotation of the zebrafish locus indicated two possible splice isoforms (ENSDART00000149878 and ENSDART00000112598), RT-PCR in 3 days post fertilization (d.p.f.) embryos showed only one of these (ENSDART00000149878) to be expressed. The MO for *otud4* targeted the donor splice site of intron 2: TACCCGAAGGAATTTGCGCACCATT.

Production of capped human mRNA

Wild-type *RNF216* (NM_207116.2) and *OTUD4* (NM_001102653.1) cDNAs were cloned into the pCR8 TOPO vector (Invitrogen). For production of capped human mRNA, the inserts were transferred to pCS2 using the Gateway technology (Invitrogen). The mutations identified in the index pedigree were introduced into *RNF216* and *OTUD4* by site-directed mutagenesis. All constructs were fully sequenced using exonic primers to verify the sequence.

Zebrafish embryo injections

All experiments were carried out with the approval of the Institutional Animal Care and Use Committee. Zebrafish were maintained and mated according to standard procedures.¹⁷ Wild-type zebrafish embryos were injected at the 1-4 cell stage with 1 nl diluted MO and 0.5% phenol red. A dose of 6 ng of *rnf216*- or *otud4*-targeting MO was used as it gave the best rate of silencing and the minimum rate of mortality among the tested working dilutions (4-10 ng). For the epistatic interaction experiments, a cocktail containing 6 ng each of *rnf216*- and *otud4*-targeting MO was used.

For RNA rescue experiments, human wild-type or mutant *RNF216* (NM_207116.2) and *OTUD4* (NM_001102653.1) were cloned into the pCS2+ expression vector and transcribed *in vitro* using the SP6 Message Machine Kit (Ambion) to produce capped mRNA, and 200 pg of mRNA was injected.

Zebrafish embryo phenotyping

Injected embryos were scored at 3 days post fertilization for microphthalmia by measuring the area of the eye cup. For immunofluorescence studies, embryos were fixed in Dent's fixative (80% methanol, 20% dimethylsulfoxide) overnight at 4 °C. After rehydration with decreasing series of methanol in PBS, the embryos were washed with PBS, permeabilized with 10 µg/ml proteinase K, and postfixed with 4% PFA. Embryos were then washed twice with IF buffer (0.1% Tween-20, 1% BSA in 1x PBS) for 10 min at room temperature. After incubation in blocking solution (10% FBS, 1% BSA in 1x PBS) for 1 h at room temperature, embryos were incubated with anti- α acetylated tubulin (1:1000 ; T7451, Sigma-Aldrich), overnight at 4°C. After two washes in IF buffer for 10 min, embryos were incubated with Alexa Fluor goat anti-mouse IgG (1:1000 ; A21207, A11001, Invitrogen) for 1 h at room temperature. Image

acquisition and analysis was performed using Nikon NIS-Elements Advanced Research software.

For each test, 50-100 embryos were injected and scored by two investigators who were blind to the injection cocktail. All experiments were performed 2-3 times and statistical significance was calculated using Student's *t*-test.

Figure S2. Allele-specific RT- PCR of *RNF216*. Quantitative real-time RT-PCR of cDNA from immortalized lymphoblast lines from Subject 5-7 and their parents who are unaffected mutation carriers. Expression was first normalized to *GAPDH* then to the expression of the mutant allele. In all cases, expression of the wild-type (WT) allele exceeded that of the mutant allele and was comparable between affected individuals and their unaffected parents.

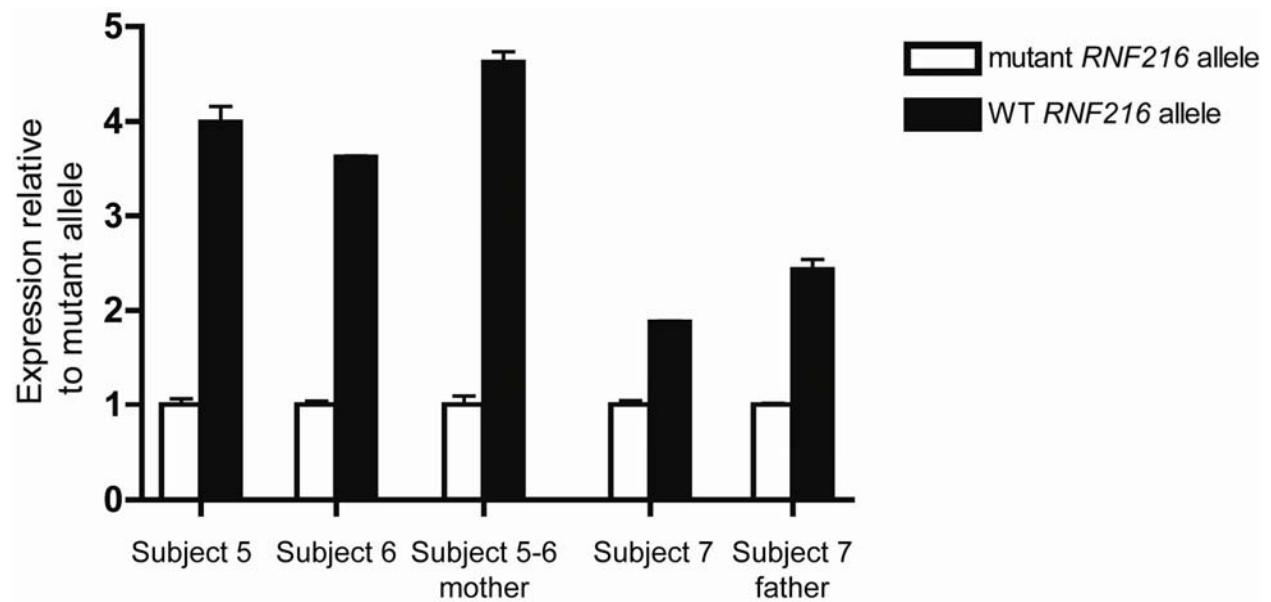


Figure S3. Efficiency of the *rnf216* and *otud4* morpholinos. Upper, amplification of the 673 base pair (bp) *rnf216* fragment spanning exons 2-7 and surrounding the exon-intron junction targeted by the *rnf216* MO reveals retention of intron 2 (77 bp in size) in the MO injected (4-10 ng) embryos (lanes 2-5). Lower, injection of the *otud4* MO (4-10 ng) reduces normal splicing of the endogenous transcript by 90% and favors aberrant splicing resulting in a transcript where intron 5 (73 bp in size) is retained.

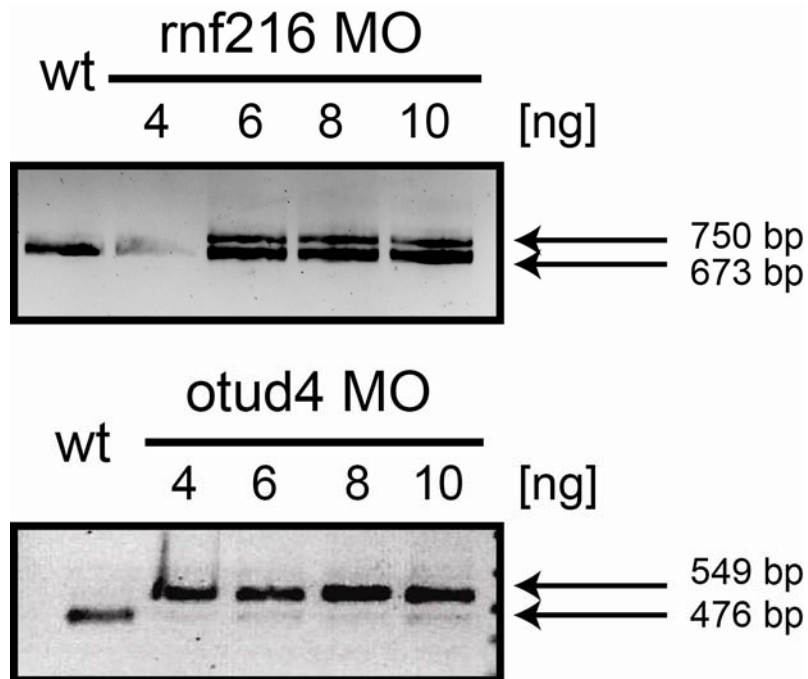


Figure S4. Combinatorial knock-down of *rnf216* and *otud4* induces microphthalmia that can be rescued by co-injection with wt human *OTUD4*. Left, Lateral views of control embryos and embryos injected with double MO (*rnf216* MO, *otud4* MO), double MO + wt human *OTUD4* and double MO + mut human *OTUD4*. Right, Measurements of the eye size area (arrows) in control embryos and embryos injected with *rnf216* MO, *otud4* MO, double MO, double MO + wt human *RNF216* double MO + mut human *RNF216*, double MO + wt human *OTUD4* double MO + mut human *OTUD4* in arbitrary units (a.u.). Data are presented as mean \pm s.e. Two-tailed *t*-tests were performed for statistical analyses. *P-value<0.05 ***P-value<0.0001

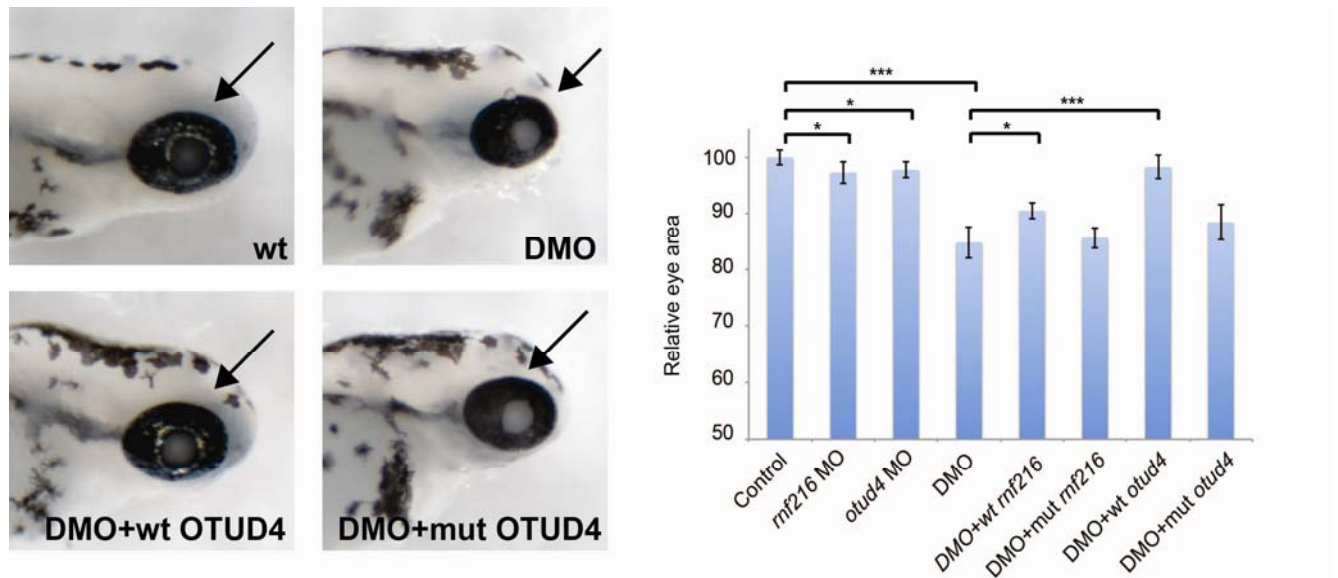


Table S1. Homozygous variants found in Subject 3 and predicted to be deleterious

Chromosome	Gene name	RefSeq Accession	Nucleotide change	Amino-acid change	Segregation with disease
1	<i>AGRN</i>	NM_198576.2	c.1123G>T	p.A375S	N
1	<i>DVLI</i>	NM_004421.2	c.997C>T	p.L333F	N
1	<i>FNDC7</i>	NM_001144937.1	c.1100A>G	p.N367S	N
1	<i>GABPB2</i>	NM_144618.2	c.439A>G	p.K147E	N
1	<i>LCE2A</i>	NM_178428.3	c.59G>A	p.C20Y	N
1	<i>OR6K2</i>	NM_001005279.1	c.236C>T	p.P79L	N
2	<i>PRPF40A</i>	NM_017892.3	c.1480-8_1480-3 delTGCTAT	splice	N
2	<i>TTC21B</i>	NM_024753.3	c.3004C>G	p.L1002V	N
2	<i>FARP2</i>	NM_014808.2	c.2185C>T	p.R729W	N
4	<i>OTUD4</i>	NM_001102653.1	c.998G>T	p.G333V	Y
7	<i>RNF216</i>	NM_207111.3	c.2251C>T	p.R751C	Y
10	<i>LOXL4</i>	NM_032211	c.1135C>T	p.R379C	N
16	<i>HYDIN</i>	NM_032821.2	c.12896G>C	p.C4299S	N

Table S2. Laboratory and genetic results for subjects

Subject	Laboratory and Genetic Studies
1	Negative genetic testing for SCA17
2	
3	Notable for type IIB hyperlipidemia After exogenous GnRH, LH rose from 0.06 IU/L to 5.8 IU/L, FSH from 0.14 IU/L to 2.0 IU/L Negative laboratory testing for disorders of glycosylation, adrenoleukodystrophy, metachromatic leukodystrophy, Krabbe and Refsum diseases, multiple sclerosis, amino acid abnormality, vitamin E deficiency Normal prolactin, cortisol, IGF-1, and thyroid studies Normal karyotype. Negative genetic testing for HD, DRPLA, FRDA, FXTAS, SBMA, SCA 1-3, 6-8, 10, 12
4	Negative for mitochondrial disorders, vitamin E deficiency, Wilson's disease, multiple sclerosis, and lysosomal storage diseases. Negative genetic testing for SCA 1,2,3,6,7, DRPLA, and HD.
5	Negative laboratory testing for lysosomal enzyme deficiency, creatine transporter deficiency, deficiency of folate, vitamin B12 or E, Tay-Sachs or Wilson's diseases, homocystinuria, fatty acid oxidation disorder, amino or organic acid abnormality, metachromatic leukodystrophy, rheumatologic disorder, multiple sclerosis, arsenic, lead, copper, or mercury poisoning Normal TSH Negative genetic testing for DRPLA, HDL2, MELAS, MERRF, NARP, SCA2, 3, and 17, normal chromosomal microarray
6	Notable for normocytic anemia and positive ANA (1:160) with homogenous pattern Negative laboratory testing for celiac, Lyme, Niemann-Pick type C, Tay-Sachs, and Wilson's diseases, syphilis, acanthocytosis, mitochondrial disorders, amino or organic acidemias, adrenoleukodystrophy, neuronal ceroid lipofuscinosis, lysosomal enzyme deficiency, lipoprotein abnormality, deficiency of coenzyme Q, folate, vitamins B12, E, or coenzyme Q Normal prolactin, TSH, cortisol Negative genetic testing for AOA1-2, AVED, DRPLA, FRDA, HD, MELAS, MERRF, MSS, NARP, SANDO, SCA1-3, 6-8, 10, 14, and 17
7	Notable for abnormal and branched mitochondria on skin biopsy, elevated pyruvate/lactate ratio, and mitochondrial enzyme studies suggestive of a complex I disorder; and a positive ANA but absence of other autoantibodies Negative laboratory testing for celiac, Lyme, Wilson's, Whipple, and Tay-Sachs diseases, hemochromatosis, syphilis, deficiency of vitamins B12 or E, amino acid abnormality, multiple sclerosis Normal prolactin, TSH, cortisol Negative genetic testing for AOA1-2, AVED, DRPLA, FRDA, MELAS, MERF, MSS, NARP, SCA 1-8, 10, 12-14, 17, 28
8	Notable for subsarcolemmal accumulation of mitochondria with complex cristae and abnormally elongated forms on muscle biopsy, mitochondrial enzyme studies suggestive of complex I-IV disorder and decreased citrate synthase activity Negative for sarcoidosis, Wilson's and celiac diseases, deficiency of vitamin E, adrenoleukodystrophy, autoimmune, peroxisomal, thyroid, liver, renal abnormalities Normal prolactin, thyroid studies, and growth-hormone and cortisol responses to arginine/insulin Normal karyotype; negative genetic testing for AOA1-2, DRPLA, FRDA, <i>POLG</i> -related disorders, SCA 1-3, 5-8, 10, 14, 17
11	Normal thyroid studies, prolactin, cortisol Normal karyotype
12	No pituitary hormone deficiencies other than hypogonadotropic hypogonadism Negative genetic testing for DRPLA, FRDA, FXTAS, MELAS, MERRF, NARP, SCA 1-3, 6-8, mitochondrial deletions

AOA, ataxia with oculomotor apraxia; AVED, ataxia with vitamin E deficiency; DRPLA, dentatorubral-pallidolusian atrophy; FRDA, Friedreich's ataxia; FXTAS, fragile X-associated tremor/ataxia syndrome; HD, Huntington's disease; HDL, Huntington's disease-like; MELAS, mitochondrial myopathy, encephalopathy, lactic acidosis, and stroke-like episodes; MERRF, myoclonic epilepsy associated with ragged red fibers; MSS, Marinesco-Sjögren syndrome; NARP, neuropathy, ataxia, and retinitis pigmentosa; SANDO, sensory ataxic neuropathy, dysarthria, and ophthalmoparesis; SBMA, spinobulbar muscular atrophy; SCA, spinocerebellar ataxia

Table S3. Known idiopathic hypogonadotropic hypogonadism (IHH) and ataxia genes used for DAPPLE, Grail, Endeavour, Inweb scored network, and CNVconnect analyses. Ataxia genes are divided into those that exhibit autosomal recessive (AR), autosomal dominant (AD), X-linked, or mitochondrial (mito) inheritance. Ataxia genes for which the genetic mutation results in expansion of triplet repeats were not included in this analysis, as these are thought to be gain-of-function mutations, and the role of endogenous gene function in the pathogenesis of ataxia with these triplet-expansion mutations is unclear.

IHH	Ataxia (AR)	Ataxia (AD)	Ataxia (X-linked)	Ataxia (mito)
<i>KAL1</i>	<i>FXN</i>	<i>SPTBN2</i>	<i>ABC7</i>	<i>TK2</i>
<i>FGF8</i>	<i>POLG</i>	<i>ATXN10</i>		<i>ATP6</i>
<i>FGFR1</i>	<i>TTPA</i>	<i>TTBK2</i>		
<i>HS6ST1</i>	<i>MTTP</i>	<i>KCNC3</i>		
<i>CHD7</i>	<i>ATM</i>	<i>PRKCG</i>		
<i>NELF</i>	<i>APTX</i>	<i>ITPR1</i>		
<i>PROK2</i>	<i>SETX</i>	<i>IFRD1</i>		
<i>PROKR2</i>	<i>HEXA</i>	<i>PDYN</i>		
<i>TAC3</i>	<i>HEXB</i>	<i>FGF14</i>		
<i>TACR3</i>	<i>PMM2</i>	<i>AFG3L2</i>		
<i>LEP</i>	<i>SACS</i>	<i>BEAN1</i>		
<i>LEPR</i>	<i>PhyH</i>	<i>TGM6</i>		
<i>KISS1</i>	<i>PEX7</i>	<i>NOP56</i>		
<i>KISS1R</i>	<i>CYP27A1</i>	<i>KCNA1</i>		
<i>GNRH1</i>	<i>SYNE1</i>	<i>CACNA1A</i>		
<i>GNRHR</i>	<i>ADCK3</i>	<i>CACNB4</i>		
	<i>NPC1</i>	<i>SLC1A3</i>		
	<i>NPC2</i>	<i>SAX1</i>		

Table S4. Primers for allele-specific PCR

RNF216 c.414delG, p.G138GfsX74 (Subjects 5-6 and family members)	
Forward	5'-GGATGACTACGGTGAATTTCTGG-3'
Reverse	5'-CACTTGGCTTAGTGAATTCAGAGATT-3'
Probe (wild-type)	5'-FAM-TCTTGGG C CTCCTGG-MGB-3'
Probe (mutant)	5'-FAM-TCTTGG C CTCCTGG-MGB-3'
RNF216 c.721C>T, p.Q241X (Subject 7 and family members)	
Forward	5'-TGGTTAGATCATCCTTACTTCCAGTC-3'
Reverse	5'-GAGGAACGACCTGGTTTGTATT-3'
Probe (wild-type)	5'-FAM-TGAACCAA C AGCCCC-MGB-3'
Probe (mutant)	5'-FAM-TGAACCAA T AGCCCC-MGB-3'

References

1. Li H, Durbin R. Fast and accurate short read alignment with Burrows-Wheeler transform. *Bioinformatics* 2009;25:1754-60
2. McKenna A, Hanna M, Banks E, et al. The Genome Analysis Toolkit: a MapReduce framework for analyzing next-generation DNA sequencing data. *Genome Res* 2010;20:1297-303
3. Exome Variant Server, NHLBI Exome Sequencing Project (ESP), Seattle, WA (URL: <http://evs.gs.washington.edu/EVS/>) [July 6, 2012].
4. Adzhubei IA, Schmidt S, Peshkin L, et al. A method and server for predicting damaging missense mutations. *Nat Methods* 2010;7:248-9.
5. Kumar P, Henikoff S, Ng PC. Predicting the effects of coding non-synonymous variants on protein function using the SIFT algorithm. *Nat Protoc* 2009;4:1073-81.
6. Mi H, Dong Q, Muruganujan A, Gaudet P, Lewis S, Thomas PD. PANTHER version 7: improved phylogenetic trees, orthologs and collaboration with the Gene Ontology Consortium. *Nucleic Acids Res* 2009;38:D204-10.
7. Schwarz JM, Rodelsperger C, Schuelke M, Seelow D. MutationTaster evaluates disease-causing potential of sequence alterations. *Nat Methods* 2010;7:575-6.
8. Rossin EJ, Lage K, Raychaudhuri S, et al. Proteins encoded in genomic regions associated with immune-mediated disease physically interact and suggest underlying biology. *PLoS Genet* 2011;7:e1001273.
9. Raychaudhuri S, Plenge RM, Rossin EJ, et al. Identifying relationships among genomic disease regions: predicting genes at pathogenic SNP associations and rare deletions. *PLoS Genet* 2009;5:e1000534.
10. Aerts S, Lambrechts D, Maity S, et al. Gene prioritization through genomic data fusion. *Nat Biotechnol* 2006;24:537-44.
11. Lage K, Mollgard K, Greenway S, et al. Dissecting spatio-temporal protein networks driving human heart development and related disorders. *Mol Syst Biol* 2010;6:381.
12. Longoni, Lage K, Russell MK, et al. Congenital diaphragmatic hernia interval on chromosome 8p23.1 characterized by genetics and protein interaction networks. *Am J Med Genet A* 158A:3148-58
13. Santen RJ, Bardin CW. Episodic luteinizing hormone secretion in man. Pulse analysis, clinical interpretation, physiologic mechanisms. *J Clin Invest* 1973;52:2617-28.
14. Hayes FJ, McNicholl DJ, Schoenfeld D, Marsh EE, Hall JE. Free alpha-subunit is superior to luteinizing hormone as a marker of gonadotropin-releasing hormone despite desensitization at fast pulse frequencies. *J Clin Endocrinol Metab* 1999;84:1028-36.
15. Spratt DI, Finkelstein JS, Badger TM, Butler JP, Crowley WF, Jr. Bio- and immunoactive luteinizing hormone responses to low doses of gonadotropin-releasing hormone (GnRH): dose-response curves in GnRH-deficient men. *J Clin Endocrinol Metab* 1986;63:143-50.
16. Seminara SB, Acierno JS, Jr., Abdulwahid NA, Crowley WF, Jr., Margolin DH. Hypogonadotropic hypogonadism and cerebellar ataxia: detailed phenotypic characterization of a large, extended kindred. *J Clin Endocrinol Metab* 2002;87:1607-12.
17. Westerfield M. *The zebrafish book: a guide for the laboratory use of zebrafish (Danio rerio)*. Eugene, OR: University of Oregon Press; 2000.